Synthesis and Fluorescence of Neodymium-Doped Barium Fluoride Nanoparticles

Christopher M. Bender and James M. Burlitch*

Department of Chemistry and Chemical Biology, Cornell University, Ithaca, New York 14853

Duane Barber and Clifford Pollock

Department of Electrical Engineering, Cornell University, Ithaca, New York 14853

Received July 27, 1999. Revised Manuscript Received April 4, 2000

Reverse microemulsions were used to synthesize barium fluoride doped with 0−65 mol % neodymium. Although the products were polydisperse, average particle sizes below 100 nm were achieved. XRD analysis showed that powders with 0−10 mol % Nd were single phase, while samples with dopant levels of 10−50 mol % contained two phases. Products with more than 50 mol % Nd were amorphous by XRD. Fluorescence of Nd:BaF_2 showed an unusually high threshold for concentration quenching as well as very short lifetimes compared to those of bulk samples. The use of a cosurfactant and variation in reaction conditions provided control over particle size; smaller particles resulted by limiting the aqueous volume while simultaneously increasing the amount of cosurfactant for a given concentration of reactants.

Introduction

Light amplification by single crystals doped with transition metals or rare earth (RE) ions is well-known. While single crystals are the most common way to amplify light, several limitations exist. Formation of large, defect-free crystals can be time-consuming and expensive, require specialized equipment, or may even be impossible for many materials. To circumvent these problems, a composite consisting of light-amplifying nanoparticles placed in a glass or polymer matrix could be used.[1]

Beecroft et al. recently described[2] chromium-doped forsterite (Cr:Mg_2SiO_4) nanoparticles embedded in a poly(tribromostyrene-*co*-naphthyl methacrylate) matrix, which showed gain of a Cr:Mg_2SiO_4 reference laser signal. Although the 5−10 μm thick waveguide composites contained only a 10 wt % loading of forsterite in the polymer, the gain was comparable to that from a single crystal of similar path length. Substantial loss, however, resulted in only slight net amplification.

While this approach is promising, there are many obstacles. To use ceramic particles, high-temperature methods are generally employed, which can lead to sintering. This may make it difficult to keep particle size below 100 nm in diameter, which is desired to avoid light scattering.[3] Like many laser crystalline materials, forsterite is biaxial. To avoid significant scattering at the crystal−matrix interface, the refractive indices must match closely. Since only one RI of a biaxial crystal can be matched by the host glass or polymer, scattering from the other two crystal faces will be unavoidable. A further constraint is that the RI must be between 1.4 and 2.2 if a titania−silica glass[4] composite is used as the host and 1.4−1.7 if a polymer[5] composite is used. Since Mg_2SiO_4 has refractive indices near 1.6, specialized polymers must be made to reach this value.

The present work explores the synthesis of nanoparticles and uses neodymium-doped BaF_2 as the optically active component. Studies by Payne et al.[6] showed that lifetimes of excited Nd in fluorite hosts were long and that these materials had potential for optical energy storage devices. Because BaF_2 is cubic, it has one refractive index (1.47),[7] and thus can be matched exactly with a glass or polymer matrix. The transparency of BaF_2 in the visible and near-IR spectral regions, as well as its stability and nonhygroscopicity, and slight solubility in water make it an attractive candidate for composite studies.

Nanoparticles of Nd:BaF_2 were synthesized by the reverse microemulsion technique. This technique was first developed by Boutonnet et al.[8] to make colloidal, zerovalent nanoparticles; the method has been exploited to include the synthesis of many different materials.[9]

In this study, various ratios of Nd^{3+} and Ba^{2+} ions were mixed with F^- ions in reverse swollen micelles

(1) Beecroft, L. L.; Ober, C. K. *Chem. Mater* **1997**, *9*, 1302−1317 and references therein.
(2) Beecroft, L. L.; Leidner, R. T.; Ober, C. K.; Barber, D. B.; Pollock, C. R. In *Better Ceramics Through Chemistry VII: Organic/Inorganic Hybrid Materials*, Coltrain, B. K., Sanchez, C., Schaefer, D. W., Wilkes, G. L., Eds.; Materials Research Society: Pittsburgh, PA, 1996; pp 575−582.
(3) Barber, D. B. Ph.D. Thesis, Cornell University, Ithaca, NY, August 1997.
(4) Brinker, C. J.; Harrington, M. S. *Sol. Energy Mater.* **1981**, *5*, 159−172.
(5) Brandrup, J.; Immergut, E. H. *Polymer Handbook, Part 2*; Wiley: New York, 1989; pp VI-453−457.
(6) Payne, S. A.; Caird, J. A.; Chase, L. L.; Smith, L. K.; Nielson, N. D.; Krupke, W. F. *J. Opt. Soc. Am. B* **1991**, *8*, 726−740.
(7) Malitson, I. H. *J. Opt. Soc. Am.* **1964**, *54*, 628−632.
(8) Boutonnet, M.; Kizling, J.; Stenius, P.; Maire, G. *Colloids Surf.* **1982**, *5*, 209−225.
(9) Pileni, M. P. *Langmuir* **1997**, *13*, 3266−3276.

10.1021/cm9904741 CCC: $19.00
Published on Web 06/23/2000

Table 1. Preparation of Nd:BaF_2[a]

prod no.	mol % Nd target (actual)[b]	reaction time (h)	salts			aq phase concn (M)				yield (%)
			NO_3	OAc	OTf	F	Ba	Nd	F	
1	0 (NA)	2.5	Ba			Na	0.30		0.65	93
2	0 (NA)	0.0	Ba			Na	0.30		0.65	92
3	12 (11)	0.75	Ba	Nd		Na	0.26	0.04	0.64	98
4	22 (19)	0.75	Ba	Nd		Na	0.22	0.11	0.64	95
5	48 (48)	0.75	Ba	Nd		Na	0.14	0.25	0.64	86
6[c]	6.1 (5.0)	2	Ba	Nd		Na	0.27	0.02	0.67	67
7	39 (25)	0.75	Ba	Nd		Na	0.17	0.10	0.64	102
8	51 (60)	0.75	Ba/Nd			Na	0.11	0.16	0.64	89
9[d]	0 (NA)	1			Ba	NH_4	0.14		0.29	91
10[d]	0 (NA)	1			Ba	NH_4	0.14		0.30	85
11[d]	0 (NA)	1			Ba	NH_4	0.14		0.30	66
12[d]	0 (NA)	1			Ba	NH_4	0.14		0.32	15

[a] Microemulsions consisted of 15 g of Igepal CO-520, 50 mL of cyclohexane, 5 mL of EtOH, and 10 mL of aqueous salt solution (Ba and Nd dissolved in the same 10 mL), unless otherwise noted. [b] Actual mole percent Nd values were determined by ICP-MS analysis. NA means not analyzed by ICP-MS. [c] Only 1 mL of cosurfactant (EtOH) was used with this procedure. [d] Methanolic microemulsion reactions (no EtOH). The volume ratio of the dispersed phase (H_2O:MeOH) was (**9**) 0:10, (**10**) 2.5:7.5, (**11**) 5.0:5.0, and (**12**) 7.5:2.5. For products analyzed by fluorescence spectroscopy, the ratios of $Ba(NO_3)_2$ to $Nd(OAc)_2$ or $Nd(NO_3)_3$ were varied such that the expected product had a mass of 0.5 g; the NaF concentration for each of these was 0.64 M.

formed by nonionic surfactants. The product was collected, and fluorescence measurements were performed to determine the optical characteristics of Nd:BaF_2 nanoparticles.

Experimental Section

Reagents. All chemicals were used as received, unless otherwise stated. Barium triflate (98%), Igepal CO-520, 49 wt % aqueous HF, $Nd(C_2H_3O_2)_3{\cdot}H_2O$ (99.9%), $Nd(NO_3)_3{\cdot}6H_2O$ (99.99%), and triflic acid (distilled before use) were obtained from Aldrich. Acetic acid (99.7%), BaF_2 (99%, for polycrystalline melt), $Ba(NO_3)_2$, NH_4F (99.9%, dried under vacuum before use), and NaF (99%) were obtained from Fisher. Methanol (distilled over magnesium) and acetone were both ACS Certified grade. Absolute ethanol was obtained from Pharmco. Barium hydroxide and NaF were obtained from Mallinckrodt. Cyclohexane (99%) was obtained from Baker. Neodymium(III) oxide (98+%) was obtained from Molybdenum Corporation of America. Water was distilled, then filtered through a Sybron/Barnstead Millipore Q system, and finally passed through ion-exchange resins to yield a product with a specific resistance of 18.6 MΩ·cm. Neodymium triflate was synthesized by previous methods.[10,11] The IR spectrum of the resulting lavender powder was in agreement with that in the literature.[12] Neodymium fluoride was synthesized by addition of 49 wt % aqueous HF (0.60 mL, 0.018 mol HF) to $Nd(OAc)_3{\cdot}H_2O$ (1.55 g, 4.57 mmol) in 15 mL of H_2O in a Teflon vial. The lavender precipitate was centrifuged (15 min, 2000 rpm) and washed with water (2 × 15 mL) and acetone (1 × 15 mL) and then dried under a heat lamp and then in a box furnace at 310 °C for 24 h. The product had the expected powder XRD pattern.[13]

A doped polycrystalline mass was made by melting BaF_2 (Fisher) and NdF_3 in a Pt crucible in a home-built graphite resistance furnace (CCMR-TOL facility). Air and moisture were eliminated from the graphite resistance furnace by first heating the sample to 250−335 °C under vacuum (10^{-5} mmHg) for 2−3 h and then back-filling with Ar.

Instrumentation. Powder XRD patterns were obtained using a Scintag PAD-X diffractometer using Cu radiation; samples were analyzed on a zero-background holder. For lattice parameter calculations, Si was used as an internal standard. IR spectra were obtained from KBr pellets using a Mattson Instrument Galaxy 4020 spectrophotometer, and were referenced against a freshly prepared blank KBr pellet. Diffuse reflectance spectra of powders under a quartz coverslip were gathered with a Shimadzu UV-3101 PC spectrophotometer. Scanning electron micrographs were made using a Leica Leo 440 microscope. Powdered samples (5−10 mg) were dispersed in 0.45 μm filtered acetone (∼2 mL) by ultrasonication for 2 min in a Branson 5200 ultrasonic bath, and allowed to dry on an Al stub. Then a ∼100 Å thick layer of Au−Pd was sputtered on to reduce charging effects. Centrifugation was carried out in either Corex glass or Nalgene bottles using an IEC-Centra-4B centrifuge. ICP-MS analysis was carried out on all Nd:BaF_2 products for which a composition is reported. For fluorescence spectroscopy, a continuous wave pump Ar laser was chopped at rates ranging from 1 to 22 kHz. The sample fluorescence was focused through a 1/4 m monochromator, and measured with a Si photodiode (rise time 10 ns). Lifetimes were determined either by direct observation of the chopped signal on an oscilloscope or indirectly using a lock-in amplifier and calculating the lifetime on the basis of the measured phase shift between the chopped pump beam and the chopped fluorescence signal.

Nanoparticle Synthesis. Following Kumar et al.,[14] microemulsions were made by dissolving 15 g of Igepal CO-520 in 50 mL of cyclohexane in a 100 mL round-bottomed flask. This mixture was stirred magnetically until it was homogeneous, and then 10 mL of an aqueous salt solution was poured in slowly. The salts were a mixture of $Ba(NO_3)_2$ or $Ba(CF_3SO_3)_2$ and neodymium acetate, nitrate, or triflate. Finally, 5 mL of EtOH (a cosurfactant) was added to the solution. In a similar fashion, a fluoride microemulsion was made in a 250 mL screw-capped Nalgene bottle by substituting 10 mL of a fluoride solution (containing NaF or NH_4F) for the barium and neodymium salt solution. These two microemulsions were allowed to stir separately for a short time (usually 2 h), and then they were combined and stirred for 0−2 h before collection of the product began. Table 1 gives the details of the syntheses.

The emulsion mixture was centrifuged at 3500−4000 rpm for 25−40 min, which caused sedimentation of the nanoparticles and allowed removal of the mother liquor. The particles were then washed and centrifuged (10 min, 3600 rpm) with portions of acetone, methanol, or ethanol (4 × 10−15 mL), dried under a heat lamp for 15−25 min, lightly crushed in an agate mortar and pestle, and then dried for an additional 5−10 min.

Nanocrystals produced by microemulsions for which methanol was the cosurfactant (methanolic microemulsions) were

(10) Roberts, J. E.; Bykowsi, J. S. *Thermochim. Acta* **1978**, *25*, 233−240.

(11) Paiva Santos, C. O.; Castellano, E. E.; Machado, L. C.; Vincentini, G. *Inorg. Chim. Acta* **1985**, *110*, 83−86.

(12) Hamidi, M. E. M.; Pascal, J.-L. *Polyhedron* **1994**, *13* (11), 1787−1792.

(13) *Powder Diffraction File [CDROM]*; International Center for Diffraction Data: Swarthmore, PA, 1993; file no. 9-416. Original: Swanson, H. E.; Gilfrich, N. T.; Cook, M. I. *Natl. Bur. Stand. (U.S.), Circ. 539* **1959**, *8*, 36.

(14) Kumar, P.; Pillai, V.; Bates, S. R.; Shah, D. O. *Mater. Lett.* **1993**, *16*, 68−74.

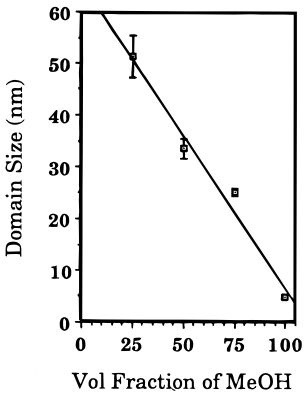

Figure 1. Domain size of BaF_2 nanoparticles (measured by XRD using the Scherrer equation) as a function of the volume fraction of methanol in a reverse microemulsion. Data are from products **9**−**12**.

made analogously to those described above, except the combined volumes of the aqueous and cosurfactant phases totaled 10 mL. Triflate salts and NH_4F were used exclusively for these studies due to their solubility in MeOH.

Results and Discussion

Synthesis. Barium fluoride was chosen as a host not only for its optical compatibility with a potential glass or polymer matrix, but also for its physical characteristics. Since BaF_2 is only slightly soluble in water, a solid was acquired in most reactions. The product was obtained after mixing the Nd^{3+}−Ba^{2+} and F^- microemulsions, allowing the solutions to react, and then collecting the product by centrifugation. The solid was washed with acetone, ethanol, or methanol to remove reaction byproducts (e.g., $NH_4CF_3SO_3$) and surfactant. The washed solid was recovered by centrifugation, dried, and analyzed.

Reactions that used dilute aqueous salt solutions (0.06 M Ba^{2+}, 0.12 M F^-) produced particle sizes below 100 nm, but gave low yields and low dopant levels (0−10% product with peaks for dopant ions not observed by reflectance spectroscopy). At higher concentration (0.3 M Ba^{2+}), enough product was obtained for analysis; however, particle size was slightly larger than 100 nm in most reactions.

Reproducible size control in the desired range was achieved only with the methanolic microemulsion reactions. In these cases, the water content of the swollen micelles was decreased while the MeOH content was simultaneously increased. Figure 1 shows dispersed phase composition and the resulting nanocrystalline domain size estimated by the Scherrer equation.[15]

For the methanolic microemulsions, it can be seen that, as the water content is decreased and the MeOH (cosurfactant) content is increased, the domain size decreases. A decrease in particle size with decreasing water-to-surfactant ratio has been observed previously;[9] however, in this study, the mass of dissolved solids remains constant. Doped products were also synthesized under these conditions, but since disorder of the crystal (e.g., by addition of Nd^{3+} into a Ba^{2+} site) would lead to broader peaks in the powder XRD pattern,[16] only undoped BaF_2 is shown in Figure 1.

(15) Cullity, B. D. *Elements of X-ray Diffraction*; Addison-Wesley: Reading, MA, 1956; p 99.

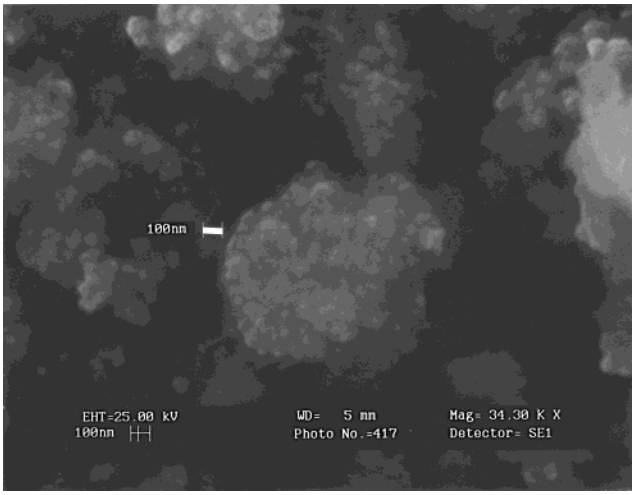

Figure 2. SEM photo of BaF_2 from a 75−25 vol % mixture of methanol−water microemulsion. The Scherrer calculated domain size of 25.2 nm is consistent with the apparent size of the particle components; however, aggregation has led to a much larger particle size.

The smaller domain size is likely due to the decreased solubility of BaF_2 in aqueous methanolic mixtures compared to pure water. Stenger found that BaF_2 had a pK_{sp} of 13.3 in methanol,[17] while Julliard et al. reported a value of 5.84 in water.[18] The decrease in solubility would lead to more rapid nucleation and reduce diffusional growth mechanisms.

Scanning Electron Microscopy. SEM was useful for qualitative assessment of the reaction products despite the inevitable aggregation of particles that occurred during sample preparation. Figure 2 shows aggregated product from a 75−25 vol % methanol−water microemulsion reaction. Though the Scherrer-calculated domain diameter (25.2 nm) is consistent with the particle component diameter observed in the photo, individual domains collectively formed a much larger particle.

Products from ethanolic microemulsion reactions contained a wide distribution of particle sizes, with most being 300 nm and larger in diameter. For reactions that produced mostly cuboidal morphologies, short reaction times (less than 2 h), use of a cosurfactant (ethanol or methanol), and low dopant levels (e.g., <1 mol % Nd) were important factors. Addition of dopants, especially at high concentrations, gave products with fewer cubes, and individual particles were often indistinguishable from one another. In these cases, size estimates by SEM were difficult.

Emulsion reactions with no dopant produced well-defined, cuboidal crystals. Figure 3A shows an electron micrograph of undoped BaF_2, **1**, produced by mixing NaF and $Ba(NO_3)_2$ microemulsions with ethanol as a cosurfactant.

Reaction time was also varied, and a product (**2**) from the synthesis with a "zero" reaction time (the microemulsions were mixed and then immediately centrifuged) had slightly smaller crystals than those from a

(16) Guinier, A. *X-ray Diffraction In Crystals, Imperfect Crystals, and Amorphous Bodies.*; W. H. Freeman: San Francisco, 1963; p 267.
(17) Stenger, V. A. *J. Chem. Eng. Data* **1996**, *41*, 1111−1113.
(18) Julliard, J.; Tissier, C.; Barczynska, J.; Mokrzan, J.; Taniewska-Osinska, S. *J. Chem. Soc., Faraday Trans. 1* **1985**, *81* (12), 3081−3090.

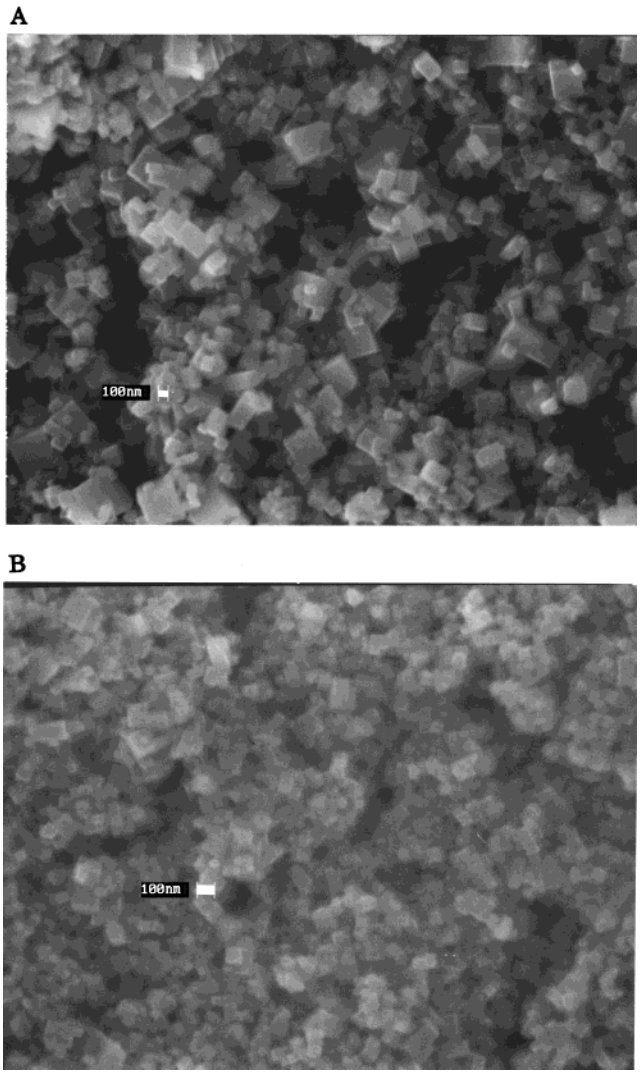

Figure 3. Scanning electron micrographs of microemulsion reaction products: (A) undoped BaF_2 (**1**) from a 2 h reaction; (B) undoped BaF_2 (**2**) collected immediately after the microemulsions were mixed. The product after 2 h is slightly larger and more polydisperse.

2 h reaction under equivalent conditions (product **1** from Table 1). Figure 3B shows that the product consisted of submicrometer-sized cubes, but they were slightly smaller. As a result, reaction times were typically kept to less than 1 h.

The synthesis of particles larger than the typical 6−60 nm given for swollen micelles[19] demonstrates that microemulsions do not consist of hard spheres that strictly limit particle growth. Particles larger than the expected swollen micelle size have been reported previously.[20] Pileni notes that an increase in the water-to-surfactant ratio increases the domain size of the product; for very high ratios (10:1 to 15:1), further particle growth ceases, but the polydispersity of the product increases.[9] Thus, it is not surprising that Nd:BaF_2 produced by microemulsions with a water-to-surfactant ratio of 16:1 is larger than expected and shows polydispersity.

(19) Hunter, R. J. *Foundations of Colloid Science*; Clarendon: Oxford, 1989; Chapter 17, pp 948−991.

(20) Monnoyer, P.; Fonesca, A.; Nagy, J. B. *Colloids Surf., A* **1995**, *100*, 233−243.

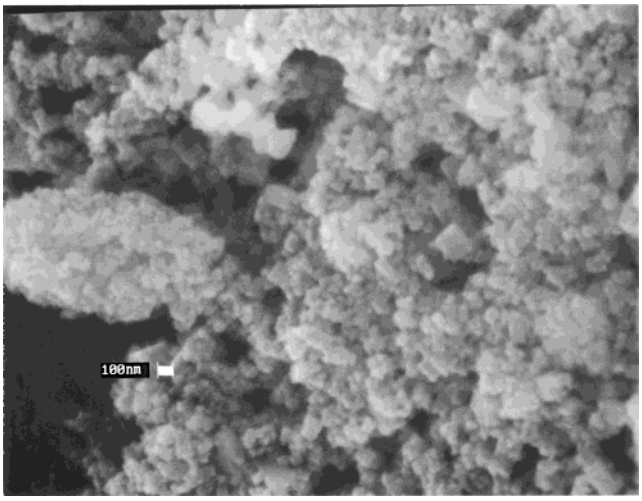

Figure 4. Nd:BaF_2 nanoparticles (**3**). As Nd (11 mol %) is added to the product, the cuboidal morphology of BaF_2 is altered.

The cuboidal product is consistent with the cubic crystal structure of BaF_2. In contrast, as dopant ions are introduced, the morphology changes, and the edges become less well-defined. Figure 4 is a micrograph of 11 mol % Nd:BaF_2 produced by mixing a $Ba(NO_3)_2$ and $Nd(OAc)_3$ microemulsion with a NaF microemulsion for 45 min. The product, while having some cube-shaped particles, is largely irregular in form. As will be discussed below, addition of dopant ions will cause changes in the host's crystal structure as well.

Powder XRD. Although an XRD pattern of a mechanical mixture of the fluorides (i.e., NdF_3 and BaF_2) showed peaks for both components, XRD patterns of microemulsion reaction products showed different results depending on Nd concentration. For products in the concentration range 0−10 mol % Nd, only peaks for single-phase BaF_2 were detected.[21] With 10−50 mol % Nd, two peaks were seen for each BaF_2 reflection. One peak appeared near the expected BaF_2 reflection, and the other was a broad peak shifted to a higher 2θ value. In the concentration range 50−65 mol % Nd, very broad peaks with low intensity and positions shifted to higher 2θ values relative to those of BaF_2 dominated the pattern. Peaks due to "pure" BaF_2 were not observed (Figure 5).

Lattice parameters of the nanosized Nd:BaF_2 were calculated using the Nelson−Riley equation.[22,23] The top line in Figure 6 represents "unshifted" peaks (data from peaks positioned where pure BaF_2 would be expected) in the 10−50 mol % range, while the bottom line represents data from the shifted peaks for this concentration range and the data from peaks in the 0−10 and 50−65 mol % ranges.

Figure 6 indicates that increasing the amount of Nd in the product results in a decrease in the calculated lattice parameter. Thus, Nd is not adhering as an adsorbed species, but is being incorporated into the

(21) *Powder Diffraction File [CDROM]*; International Center for Diffraction Data: Swarthmore, PA, 1993; file no. 4-452. Original: Swanson, H. E.; Tatge, E. *Natl. Bur. Stand. (U.S.), Circ. 539* **1953**, *1*, 70−73.

(22) Nelson, J. B.; Riley, D. P. *Proc. Phys. Soc. (London)* **1945**, *57*, 160−177.

(23) Taylor, A.; Sinclair, H. *Proc. Phys. Soc. (London)* **1945**, *57*, 126−135.

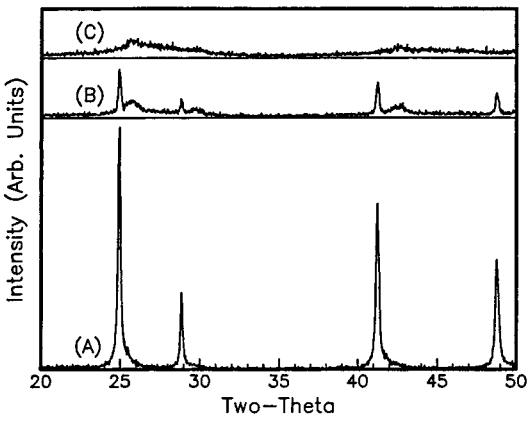

Figure 5. Powder XRD patterns of Nd:BaF_2 from reverse microemulsion reactions: (A) single-phase product **6** (5.0 mol % Nd); (B) from **7** (25 mol % Nd), which apparently contains two phases (BaF_2 and a solid solution of Nd in BaF_2); (C) from **8** (60 mol % Nd), which shows little or no crystallinity.

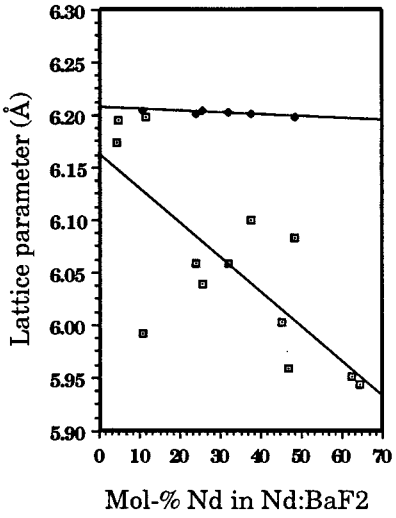

Figure 6. Correlation of lattice parameters (as determined by the Nelson−Riley formula) and mole percent Nd in BaF_2 (analyzed by ICP-MS). The top line represents lattice parameters derived from the unshifted peaks in the concentration range 10−50 mol %. The bottom line represents lattice parameters derived from peaks in the 0−9 and 50−65 mol % ranges, as well as the shifted peaks in the 10−50 mol % range.

structure of the BaF_2. A shift in lattice parameter would not be observed if substitution was not occurring. Because peaks for NdF_3 are not seen in the XRD patterns, the data also suggest that the product is not a core of NdF_3 surrounded by BaF_2 or nanocrystals of NdF_3 embedded in BaF_2. Instead, a decrease in lattice parameters correlates with an increase in Nd concentration. This is precisely the expected result since eight-coordinate Nd^{3+} has an atomic radius of 1.26 Å,[24] while eight-coordinate Ba^{2+} has an atomic radius of 1.56 Å.[24] Thus, in accordance with Vegard's law,[15] the cubic lattice parameter of Nd:BaF_2 will shrink relative to that of pure BaF_2 on incorporation of Nd^{3+}.

Another important observation is the presence of shifted and unshifted peaks in the same XRD pattern; above a Nd^{3+} concentration threshold of ∼10 mol %, some crystallites appear to have significant amounts of Nd, while others have very little or none. Also, in the cases of high Nd levels, the shifted peaks broaden and may lose intensity. This could mean the crystallites are very small, there is a large range of concentrations in different BaF_2 crystals, or the extent of disorder is large, or some combination of these.

A disordered product would be expected if enough defects occurred to distort the normal crystal structure. Since Nd is trivalent and Ba is divalent, the need for charge compensation via a defect in the crystal structure arises.[25] Under conditions of single-crystal growth, this is accomplished by filling a nearby interstitial site with a fluoride,[6] but since the microemulsion syntheses are carried out in water, OH^- or O^{2-} ions could fill the interstitial sites to compensate. Due to their size, other anions present, namely, NO_3^-, OAc^-, or triflate, would be too large to substitute at a fluoride interstitial site. With a high concentration of neodymium ions in a crystal and a large number of defects imposed, it is conceivable that the nanocrystals could lose the rigid fluorite structure, and appear amorphous by XRD.

Small crystals could be expected if the reactants are mixed rapidly. A high rate of nucleation would inhibit growth by using up available starting material. Because the grain boundary becomes indistinguishable with high dopant levels, grain size is difficult to measure by SEM. As noted earlier, the Scherrer domain size would also be difficult to correctly ascertain since the Nd dopant could broaden the reflections due to the defects discussed above.

As for variable concentrations of Nd in BaF_2 crystallites, it is known that NdF_3 and BaF_2 have different solubilities. In water, the solubility of BaF_2 is 7.1×10^{-3} M,[18] while the solubility[26] of NdF_3 is 6.7×10^{-6} M. An inhomogeneous product results if neodymium fluoride precipitates more quickly due to its insolubility;[27] the first crystallites formed would contain a higher proportion of Nd relative to crystals formed later. Crystals formed after the initial precipitation would be relatively free of Nd, and would produce the unshifted peaks in the XRD patterns.

It is also possible that a concentration gradient could occur within the particles. As Nd precipitated, the inner core of the particles would be enriched with Nd, and after the solution became depleted of Nd, BaF_2 would precipitate using Nd:BaF_2 as a "primary particle" for growth.

In cases where there were two peaks in the XRD pattern, there was a difference between crystals with a low Nd concentration ("unshifted" peaks) and those with considerable Nd concentration. Note, however, that the unshifted peaks have higher 2θ values relative to those of pure BaF_2, and show the same trend in lattice parameter as the shifted peaks, though to a much smaller degree. Thus, it seems likely that there was some Nd incorporation into these crystals as well.

Sodium fluoride was the only impurity detected in the product by XRD. In cases where a large excess of NaF

(24) Shannon, R. D.; Prewitt, L. T. *Acta Crystallogr., Sect. B* **1969**, *25*, 925−946.

(25) Andeen, C. G.; Fontanella, J. J.; Wintersgill, M. C.; Welcher, P. J.; Kimble, R. J.; Mathews, G. E. *J. Phys. C.: Solid State Phys.* **1981**, *14*, 3557−3574.

(26) Itoh, H.; Hachiya, H.; Tsuchiya, M.; Suzuki, Y.; Asano, Y. *Bull. Chem. Soc. Jpn.* **1983**, *57*, 1689−1690.

(27) Fiebush, A. M.; Rowley, K.; Gordon, L. *Anal. Chem.* **1958**, *30* (10), 1605−1609.

Table 2. Rare Earth Ion Absorptions and Emissions from Nd:BaF_2

peak observed (nm)	expected value (nm)[31]	assigned transition[6,32]	peak observed (nm)	expected value (nm)[31]	assigned transition[6,32]
350[a]	354	$^4I_{9/2} \rightarrow {}^4D_{3/2}$	795[a]	798	$^4I_{9/2} \rightarrow {}^2H_{9/2}$
523[a]	522	$^4I_{9/2} \rightarrow {}^4G_{7/2}$	800[a]	803	$^4I_{9/2} \rightarrow {}^4F_{5/2}$
572[a]	574	$^4I_{9/2} \rightarrow {}^4G_{5/2}$	864[a]	868	$^4I_{9/2} \rightarrow {}^4F_{3/2}$
733[a]	740	$^4I_{9/2} \rightarrow {}^4S_{3/2}$	~1052[e]	~1060	$^4F_{3/2} \rightarrow {}^4I_{11/2}$
746[a]	742	$^4I_{9/2} \rightarrow {}^4F_{7/2}$			

[a] Absorption. [e] Emission.

was used, peaks from crystalline NaF could be found at 39° (2θ) for the intense (200) reflection.[28] For other fluoride salts used (e.g., potassium, rubidium, cesium, or ammonium), crystalline impurities were not detected, even when large excesses were used. The NaF impurity can be avoided by using stoichiometric amounts of reactants, or a more soluble substitute for NaF can be used, e.g., KF, RbF, CsF, or NH_4F.

Reflectance Spectroscopy. Diffuse reflectance spectroscopy was used to qualitatively analyze for rare earth ions in the products. Since BaF_2 has no transitions in the region of interest (200−1400 nm) under normal conditions (i.e., those not concerned with cross luminescence),[29] any peaks would be due to impurities, dopants, or instrumental features. Table 2 shows the major absorptions for Nd:BaF_2 and those found in the literature for Nd. A peak was also found at 277 nm which was attributed to the surfactant. The phenyl ring of Igepal CO-520 acted as the chromophore.[30] Elemental analysis indicated that 2.5−3 wt % of the products was carbon-based material, most likely surface-bound surfactant.

Reflectance was useful for qualitative detection of rare earth ions. While obtaining precise dopant levels from reflectance would be difficult, general trends could be ascertained. Products with a higher level of dopant showed a corresponding increase in peak height in the reflectance spectrum.

IR Spectroscopy. IR spectra were used to determine whether surfactant was removed from the product after washing by noting characteristic absorption bands for the alkyl and phenyl groups in the C−H stretching region (2900−3100 cm^{-1}). The presence of byproduct ions, notably, nitrate, acetate, and triflate, was revealed by characteristic absorptions.

IR analysis conclusively showed that anions were not passive spectators in the reactions, but were incorporated into the product.

When nitrate salts were used, even if only for the dopant, the NO_2 asymmetric stretching vibration[33] for NO_3^- was clearly visible in the IR spectrum at 1385 cm^{-1} (lit.[34] 1385 cm^{-1} for $NaNO_3$). Elemental analysis for nitrogen of Nd:BaF_2 powders produced with Ba$(NO_3)_2$ and Nd$(NO_3)_3$ indicated that up to 3 wt % of the sample could be nitrate. Samples in which Nd$(NO_3)_3$ was the only nitrate source had lower levels (below the 0.5 wt % N detection limit). If acetate were substituted for NO_3^-, it could be seen as well with peaks at 1555 and 1439 cm^{-1} (lit.[35] 1578 s and 1435 s cm^{-1}). Finally, triflate anions have been tried, but thorough washing in a solvent with a high dielectric constant (e.g., MeOH) was needed to purify the product. Triflate is advantageous from the standpoint that it is noncomplexing, its salts are highly soluble, and it is significantly larger than F^-. Thus, incorporation of $CF_3SO_3^-$ into the BaF_2 lattice should be unlikely. Water, or possibly hydroxyl groups, was also found to be present in as-prepared powders as shown by strong absorptions at 3400 and 1600 cm^{-1} indicative of antisymmetric and symmetric stretches and HOH bending modes.[36]

Fluorescence Spectroscopy. Using an Ar ion laser (λ_{max} of 488 nm), samples of Nd:BaF_2 were examined for fluorescence. The emission spectrum of the powders showed a λ_{max} at 1052 nm, comparable to that found for Nd-doped fluoride hosts.[6] The measured lifetimes were extremely short compared to lifetimes found in bulk samples. Typical values of Nd-doped oxide, fluoride, phosphate, tungstate, etc. single crystals studied at 300 K most often had dopant levels of 0.5−2 wt % and showed lifetimes from 0.1 to 1.25 ms[37] (nearly all were <1 ms). Payne et al. reported a 4.5 ms emission lifetime for single crystalline Nd:BaF_2 (~0.2 wt % Nd).[6] This contrasts strongly with the lifetimes of nanocrystals in this study, which were on the order of 350−900 ns. There was no apparent correlation between lifetime and dopant concentration or anion impurities. One exception to the extremely short lifetimes was found with product **3** in Table 1 (11 mol % Nd by ICP analysis), which showed a long, faint tail out to 3500 ns.

A polycrystalline mass, synthesized by melting BaF_2 and NdF_3 (5 mol % Nd by ICP analysis), showed two decay processes. One lifetime was found to be ~3000 ns, while a much slower decay process had a lifetime of ~11 000 ns. Particle size could not account for the longer lifetime in the polycrystalline mass because a powdered sample of this material, produced by grinding, gave roughly the same lifetimes as the intact polycrystalline mass.

(28) *Powder Diffraction File [CDROM]*; International Center for Diffraction Data: Swarthmore, PA, 1993; file no. 36-1455. Original: McMurdie, H. F.; Morris, M. C.; Evans, E. H.; Paretzkin, B.; Wong-Ng, W.; Ettlinger, L.; Hubbard, C. R. *Powder Diffr.* **1986**, *1* (2), 74.

(29) Blaisse, G.; Grabmaeir, B. C. *Luminescent Materials*; Springer-Verlag: Berlin, 1994; p 188.

(30) Meszlenyi, G.; Kortvelyessy, J.; Juhasz, E.; Eros-Lelkes, M. *Period. Polytech., Chem. Eng.* **1986**, *30* (3, 4), 171−175.

(31) Moeller, T. In *The Rare Earths*, Spedding, F. H., Daane, A. H., Eds.; John Wiley & Sons: New York, 1961; pp 9−28.

(32) Dieke, G. H. *Spectra and Energy Levels of Rare Earth Ions in Crystals*; John Wiley & Sons: New York, 1968; p 142.

(33) Field, B. O.; Hardy, C. J. *Q. Rev., Chem. Soc.* **1964**, *18*, 361−388.

(34) Buijs, K.; Schutte, C. J. H. *Spectrochim. Acta* **1962**, *18*, 307−313.

(35) Grigor'ev, A. I. *Zh. Neorg. Khim. (Engl. Trans.)* **1963**, *8*, 409−414.

(36) Nakamoto, K. *Infrared and Raman Spectra of Inorganic and Coordination Compounds*; John Wiley and Sons: New York, 1978; p 227.

(37) Moulton, P. F. In *CRC Handbook of Laser Science and Technology (Vol. 1 Lasers and Masers)*, Weber, M. J., Ed.; CRC: Boca Raton, FL, 1982; pp 75−101.

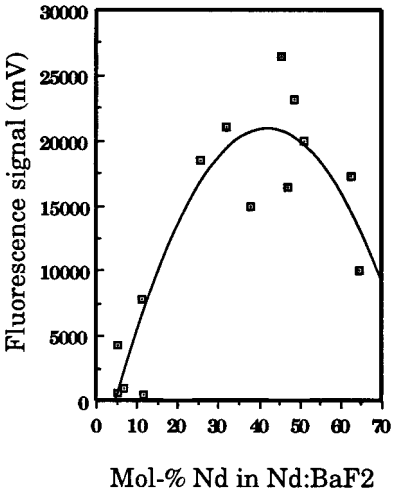

Figure 7. Fluorescence signal at 1052 nm versus mole percent Nd in Nd:BaF_2. The decrease in intensity at very high dopant levels is attributed to concentration quenching.

Others have reported[38,39] a two-decay process for Nd^{3+} in SiO_2 glass, in which Nd tended to cluster, giving rise to a fast decay component (FDC) of ~0.35 μs and a slow decay component of ~470 μs; addition of Al_2O_3 or P_2O_5 to the melt eliminated the FDC entirely. Typically, a molar ratio of 8:1 and 15:1 for Al:Nd and P:Nd, respectively, gave the best results while not modifying the properties of the silica glass. Although the study did not find conclusive evidence as to why doping had this effect, it was suggested that the added ions helped in dispersing clusters of Nd ions by a solvation mechanism.

At very high dopant levels there was a decrease in fluorescence intensity (Figure 7). Concentration quenching is a common loss mechanism for active laser centers;[40] however, this phenomenon would be expected to occur at much lower concentrations. In Nd:YAG single crystals, concentrations greater than ~1 wt % (6 atom %)[45] show a loss of signal. Although a concentration quenching study on Nd:BaF_2 has not been reported, Payne et al. reported that clustering was observed in single-crystal samples of SrF_2 with concentrations greater than 0.20 atom % Nd.[6] Andeen et al.[25] observed that rare earth ion doping at levels of 0.20 mol % in BaF_2 showed clusters dominating when optical studies were used; however, other methods (dielectric spectra) showed clustering at levels near 1.0 mol % for rare earth ions.

Concentration quenching can be suppressed by providing specific structural units in the host lattice, thereby separating the Nd ions. For instance, Bondar et al.[42,43] report suppressed concentration quenching with a neodymium-doped pentaphosphate single crystal. The phosphates may act as spacers between Nd atoms, so concentration quenching occurs at a higher concentration of Nd. In BaF_2 no such spacers exist, so that quenching would be expected to occur at a much lower Nd concentration than was observed in this study.

It is generally observed, however, that glasses can be doped with higher levels of Nd than single crystals. Koechner reports[44] that Nd doped in glass is typically used at levels of about 3 wt %. An increased level of dopant concentration could be due to the amorphous structure of the glass. In a crystal, the Nd ions will be located at specific substitutional sites and will have a tendency to cluster. In the amorphous structure of glass, however, Nd can undergo a more random substitution without causing much strain. Since the X-ray powder patterns suggest that the BaF_2 crystal structure is being lost at higher concentrations of Nd, this may explain the delay in fluorescence signal loss.

Another mechanism that may account for the delay in fluorescence quenching could be due to the nanosized particles. It is speculated that Nd atoms on the surface of the nanoparticle may have fluorescence properties different from those in the bulk. It is known that atoms on the surface do not have a full coordination sphere, and this leads to surface atoms having a higher potential energy.[45] Because nanoparticles have a higher proportion of surface atoms to bulk atoms than do larger particles, more Nd atoms would reside at the surface of a nanoparticle. The incomplete coordination sphere of the surface atoms could result in Nd atoms that promote radiative decay, rather than nonradiative decay, mechanisms.

Conclusions

Microemulsions have been used to make nanosized domains of Nd:BaF_2. The control of domain size exhibited by the methanolic microemulsions shows this method has much potential for making nanosized crystals in the desired size regime. Furthermore, size is not limited to one value, since a simple change in parameters allows control over domain size.

Obtaining nanocrystals free from impurities has been a challenge; the high surface area of the nanoparticles promotes adsorption. The use of noncomplexing salts ($CF_3SO_3^-$) and washing in high dielectric solvents have been advantageous in this regard.

While the XRD patterns showed 0−10 mol % Nd:BaF_2 consisted of single-phase product, powders produced in the 10−50 mol % range showed at least two phases were present. From plots of lattice parameter as a function of dopant level, the extra peaks were found to be a solid solution of Nd in BaF_2 with a decrease in lattice parameter correlated with an increase in Nd concentration. Products doped >50 mol % were found to be nearly amorphous by XRD.

The fluorescence properties of the Nd:BaF_2 also open up interesting questions. Short lifetimes of Nd:BaF_2 were observed, probably due to Nd clustering. Quenching of fluorescence intensity was not observed until very high dopant levels compared to other literature values, and may be due to the disruption of the rigid crystalline structure in favor of a more disordered one. Another

(38) Arai, K.; Namikawa, H.; Kumata, K.; Ishi, Y.; Tanaka, H.; Ida, I. *Jpn. J. Appl. Phys. (Pt. 2, Lett.)* **1983**, *22*, L397−L399.
(39) Arai, K.; Namikawa, H.; Kumata, K.; Honda, T.; Ishii, Y.; Handa, T. *J. Appl. Phys.* **1986**, *59*, 3430−3436.
(40) Chinn, S. R. In *CRC Handbook of Laser Science and Technology (Vol. 1, Lasers and Masers)*, Weber, M. J., Ed.; CRC: Boca Raton, FL, 1982; pp 149−150.
(41) Geusic, J. E.; Marcos, H. M.; Van Uitert, L. G. *Appl. Phys. Lett.* **1964**, *4*, 182−184.
(42) Bondar, I. A.; Denker, B. I.; Domanskii, A. I.; Mamelov, T. G.; Mezentseva, L. P.; Osiko, V. V.; Shcherbakov, I. A. *Sov. J. Quantum Electron.* **1977**, *7*, 167−171.
(43) Danielmeyer, H. G.; Weber, H. P. *IEEE J. Quantum Electron.* **1972**, *QE-8*, 805.
(44) Koechner, W. *Solid-State Laser Engineering*; Springer-Verlag: New York, 1976; p 61.
(45) Kuznetsov, V. D. *Surface Energy of Solids (Engligh Translation)*; Her Majesty's Stationary Office: London, 1957; Chapter 1.

reason may be the increased number of Nd atoms on the surface, which may radiatively decay differently than bulk atoms.

Acknowledgment. Thanks are due to Maura Weathers for helpful discussions on XRD data, John Hunt for help with SEM photographs, Gerhard Schmidt for synthesis of the polycrystalline Nd:BaF_2 mass, and Mike Cheatham for ICP measurements. This research was supported by a grant from the Center for Materials Research at Cornell University (NSF, DMR 9121654).

CM9904741